

# Simulation of Buffer Current Effects on Breakdown Voltage in AlGaIn/GaN HEMTs Having Passivation Layers with Different Permittivity

Y. Satoh, H. Hanawa and K. Horio

Faculty of Systems Engineering, Shibaura Institute of Technology  
307 Fukasaku, Saitama 337-8570, Japan, horio@sic.shibaura-it.ac.jp

## ABSTRACT

A two-dimensional simulation of off-state breakdown characteristics in AlGaIn/GaN HEMTs is performed, with the relative permittivity of passivation layer  $\epsilon_r$  as a parameter. The simulation is made with and without impact ionization of carriers to study how the buffer leakage current affects the breakdown characteristics. It is shown that when  $\epsilon_r$  is low, the breakdown voltage is determined by the impact ionization of carriers, and when  $\epsilon_r$  becomes high, it is determined by the buffer leakage current. This buffer leakage current decreases as  $\epsilon_r$  increases because the electric field at the drain edge of the gate is weakened, and hence the breakdown voltage increases as  $\epsilon_r$  increases.

**Keywords:** GaN HEMT, breakdown voltage, passivation layer, buffer leakage current, two-dimensional analysis

## 1 INTRODUCTION

AlGaIn/GaN HEMTs are now receiving great attention because of their applications to high-frequency power devices and high-power switching devices [1, 2]. It is known that the introduction of a gate field plate improves the power performance of AlGaIn/GaN HEMTs [3-5]. This is because it can reduce so-called current collapse [6, 7] and also enhance the off-state breakdown voltage [8-10]. The enhancement of the breakdown voltage occurs because the electric field around the drain edge of the gate is reduced by introducing the field plate [8, 10]. However, the field plate increases a gate parasitic capacitance. Therefore it may lead to the degradation of the high frequency performance

As another way to improve the breakdown voltage, introducing a passivation layer with high permittivity can also be considered [11, 12]. In fact, the introduction of a high- $k$  layer can smooth electric field profiles between the gate and the drain [13]. The high- $k$  dielectric is studied as a gate insulator in GaN-based MISHEMTs as well as Si MOSFETs. For example, HfO<sub>2</sub> (relative permittivity:  $\epsilon_r \sim 20$ ), La<sub>2</sub>O<sub>3</sub> ( $\epsilon_r \sim 27$ ) and LaLuO<sub>3</sub> ( $\epsilon_r \sim 28$ ) etc. are studied in AlGaIn/GaN MISHEMTs [14, 15]. In previous works [11, 12], we considered the high- $k$  dielectric only as a passivation layer and calculated off-state breakdown characteristics of AlGaIn/GaN HEMTs as a parameter of the passivation layer's relative permittivity  $\epsilon_r$ , and showed that the breakdown voltage increased with  $\epsilon_r$ . But we calculated only the case with impact ionization, and it was

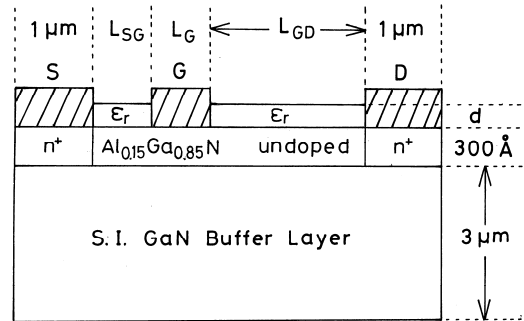


Figure 1: Device structure analyzed in this study.

not clear how the buffer leakage current affected the breakdown voltage. Therefore, in this work, we simulate the off-state drain current - drain voltage characteristics of AlGaIn/GaN HEMTs as a parameter of  $\epsilon_r$  with and without impact ionization, and particularly study how the buffer leakage current affects the off-state breakdown voltage.

## 2 PHYSICAL MODELS

Figure 1 shows a device structure analyzed in this study. The gate length  $L_G$  is 0.3  $\mu\text{m}$  and the gate-to-drain distance  $L_{GD}$  is 1.5  $\mu\text{m}$ . The thickness of passivation layer  $d$  is 0.1  $\mu\text{m}$ . The relative permittivity of the passivation layer  $\epsilon_r$  is varied between 4.2 and 60. Here, we don't include gate tunneling [8, 10]. We consider the breakdown due to an increase in the buffer leakage current or due to the impact ionization of carriers. In a semi-insulating buffer layer, we consider a shallow donor, a deep donor, and a deep acceptor [16-18]. As an energy level of the deep acceptor, we consider  $E_C - 2.85 \text{ eV}$  ( $E_V + 0.6 \text{ eV}$ ). For impurity compensation, we consider  $E_C - 0.5 \text{ eV}$  as an energy level of the deep donor. The deep-acceptor density  $N_{DA}$  is set rather high of  $10^{17} \text{ cm}^{-3}$ . A study [19] indicates that to reduce short-channel effects, an acceptor density in a buffer layer should be higher than  $10^{17} \text{ cm}^{-3}$ . Basic equations to be solved are Poisson's equation including ionized deep-level terms and continuity equations for electrons and holes including a carrier generation rate by impact ionization and carrier loss rates via the deep levels [10, 20-22]. These equations are expressed as follows.

1) Poisson's equation

$$\nabla \cdot (\epsilon \nabla \psi) = -q(p - n + N_{DI} + N_{DD}^+ - N_{DA}^-) \quad (1)$$

2) Continuity equations for electrons and holes

$$\nabla \cdot \mathbf{J}_n = -qG + q(R_{DD} + R_{DA}) \quad (2)$$

$$\nabla \cdot \mathbf{J}_p = qG - q(R_{DD} + R_{DA}) \quad (3)$$

where  $N_{DD}^+$  and  $N_{DA}^-$  are the ionized deep-donor and deep-acceptor densities, respectively.  $R_{DD}$  and  $R_{DA}$  represent carrier recombination rates via the deep donors and the deep acceptors, respectively.  $G$  is a carrier generation rate by impact ionization, and given by

$$G = (\alpha_n |J_n| + \alpha_p |J_p|) / q \quad (4)$$

where  $\alpha_n$  and  $\alpha_p$  are ionization rates for electrons and holes, respectively, and expressed as

$$\alpha_n = A_n \exp(-B_n / |E|) \quad (5)$$

$$\alpha_p = A_p \exp(-B_p / |E|) \quad (6)$$

where  $E$  is the electric field.  $A_n$ ,  $B_n$ ,  $A_p$ , and  $B_p$  are deduced from [23].

The above basic equations are put into discrete forms and solved numerically.

### 3 CALCULATED RESULTS AND DISCUSSIONS

Figure 2 shows calculated  $I_D$ - $V_D$  curves of AlGaIn/GaN HEMTs as a parameter of the relative permittivity of the passivation layer  $\epsilon_r$ . Here, the gate voltage  $V_G$  is  $-8$  V and it is an off state. The solid lines correspond to the cases with impact ionization, and the dashed lines correspond to the cases without impact ionization. The drain currents calculated without impact ionization are normal buffer leakage currents [24, 25], which are determined by buffer trapping. They are clearly seen to be lower for higher  $\epsilon_r$ . This is because the electric field at the drain edge of the gate is reduced in the case of higher  $\epsilon_r$ . When  $\epsilon_r$  is low ( $< 20$ ), an abrupt increase in  $I_D$  due to impact ionization of carriers determines the off-state breakdown voltage  $V_{br}$ . On the other hand, when  $\epsilon_r$  is high ( $\geq 30$ ), the buffer leakage current reaches a critical value (1 mA/mm) before the abrupt increase in  $I_D$ , and it determines  $V_{br}$ . Here, the off-state breakdown voltage  $V_{br}$  is defined as a drain voltage when  $I_D$  becomes 1 mA/mm, and the breakdown voltage becomes higher when  $\epsilon_r$  is higher.

Figure 3 shows the electric field profiles along the AlGaIn/GaN heterojunction interface when  $\epsilon_r$  are different. When  $\epsilon_r$  is 4.2, an increase in  $V_D$  is almost applied along the drain edge of the gate, resulting in the abrupt increase in  $I_D$  around  $V_D = 55$  V (Fig.2). However, as seen in Fig. 3(b), when  $\epsilon_r$  becomes 30, the electric field at the drain edge of the gate is reduced, and it is not so high at  $V_D = 50$  V. As  $V_D$  increases, the electric field between the gate and the drain increases, and the electric field near the drain begins to become high around  $V_D = 200$  V. Then, the electric field at the drain edge of the gate also becomes rather high at  $V_D = 301$  V, which is the breakdown voltage. Note that in this case, real gate breakdown occurs around  $V_D = 360$  V, as seen in Fig.2. Therefore, the buffer leakage current reaches the critical value before the electric field at the drain edge

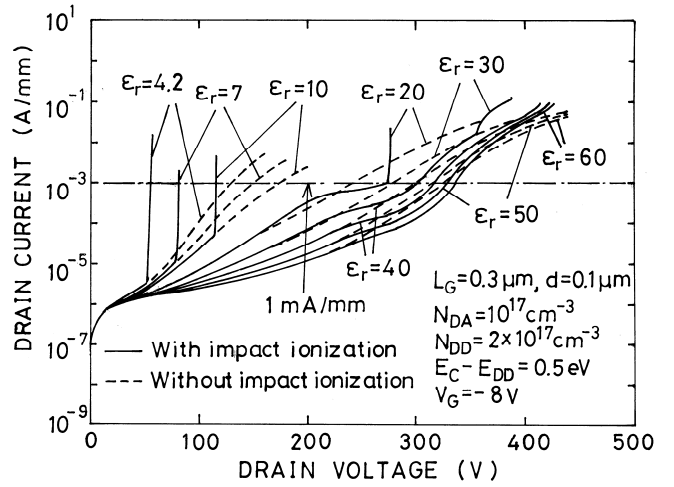


Figure 2: Calculated  $I_D - V_D$  curves of AlGaIn/GaN HEMTs as a parameter of  $\epsilon_r$ .  $V_G = -8$  V.  $L_{GD} = 1.5$   $\mu\text{m}$  and  $d = 0.1$   $\mu\text{m}$ .

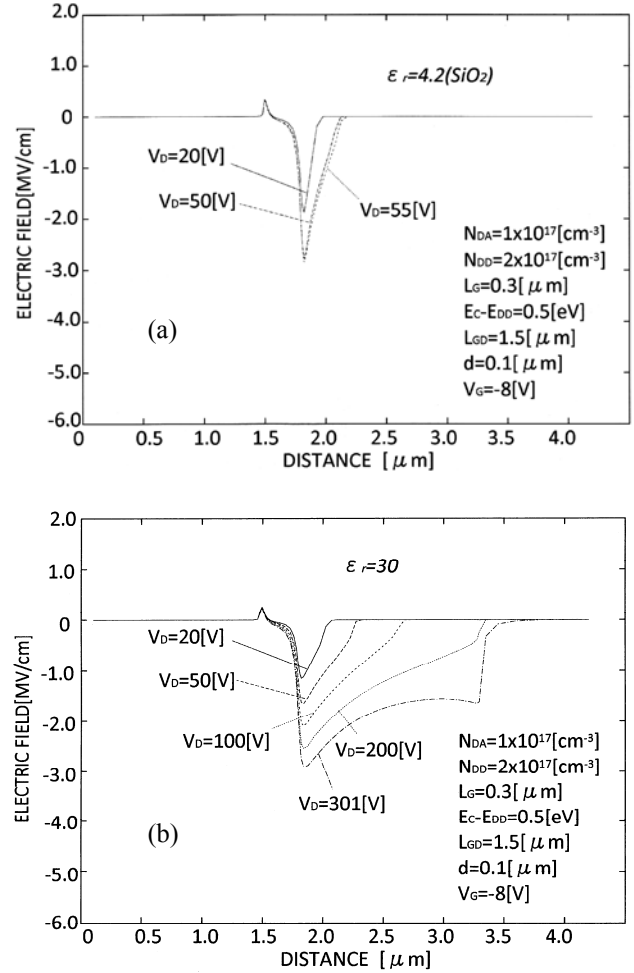


Figure 3: Electric field profiles along the heterojunction interface, with  $V_D$  as a parameter.  $V_G = -8$  V. (a)  $\epsilon_r = 4.2$ , (b)  $\epsilon_r = 30$ .  $d = 0.1$   $\mu\text{m}$ .

of the gate reaches the theoretical breakdown field of GaN ( $\geq 3$  MV/cm).

Here, it should be mentioned that the  $I_D$ - $V_D$  curves show complex features when  $\epsilon_r$  is relatively high, that is,  $I_D$  with impact ionization takes both a lower and a higher value than that without impact ionization. This is originated from the fact that holes are generated by impact ionization between the gate and the drain and they flow into the buffer layer. These holes are captured by traps, modulating potential profiles around the channel-buffer interface and affecting electron injection into the buffer layer. Electron densities as well as hole densities are increasing in the buffer layer [12, 13]. Therefore, the traps become acting as recombination centers, and hence the barrier for electrons toward the buffer raises at the drain side of the gate region to make the drain current lower than that without impact ionization [20]. On the other hand, the barrier for electrons at the source side decreases by hole trapping, resulting in the increase in the drain current and making the drain current higher than that without impact ionization particularly at high  $V_D$ . Similar features mentioned above were discussed in detail before in the case of GaAs MESFETs on a semi-insulating substrate [20].

Figure 4 shows calculated  $I_D$ - $V_D$  curves of AlGaIn/GaN HEMTs when  $V_G$  is  $-10$  V, with the relative permittivity of the passivation layer  $\epsilon_r$  as a parameter. In this case  $V_G$  is more negative than in Fig.2. The solid lines correspond to the cases with impact ionization, and the dashed lines correspond to the cases without impact ionization. The drain currents calculated without impact ionization are lower than those in Fig.2, which indicates that the buffer leakage currents become lower for the case of  $V_G = -10$  V. This is because the depletion layer extends more into the buffer layer. Figure 5 shows  $V_{br}$  versus  $\epsilon_r$  for the two cases with  $V_G = -8$  V and  $-10$  V. When  $V_G = -10$  V,  $V_{br}$  becomes lower when  $\epsilon_r$  is low ( $< 20$ ). This is because the electric field at the drain edge of the gate is higher when  $V_G$  is more negative and the breakdown due to the impact ionization of carriers occurs at lower  $V_D$ . On the other hand,  $V_{br}$  becomes higher in the region where  $\epsilon_r$  is high ( $\geq 30$ ). This is because when the gate voltage is more negative, the depletion region extends more into the buffer layer, and hence the buffer leakage current becomes smaller. Thus, the breakdown voltage determined by the buffer leakage current becomes higher.

#### 4 CONCLUSION

A two-dimensional simulation of off-state breakdown characteristics in AlGaIn/GaN HEMTs has been performed with and without impact ionization by considering a deep donor and a deep acceptor in the semi-insulating buffer layer. It has been shown that the buffer leakage current decreases as the relative permittivity of passivation layer  $\epsilon_r$  increases, because the electric field at the drain edge of the gate is reduced. When  $\epsilon_r$  is low, the impact ionization of carriers determines the off-state breakdown voltage. On the

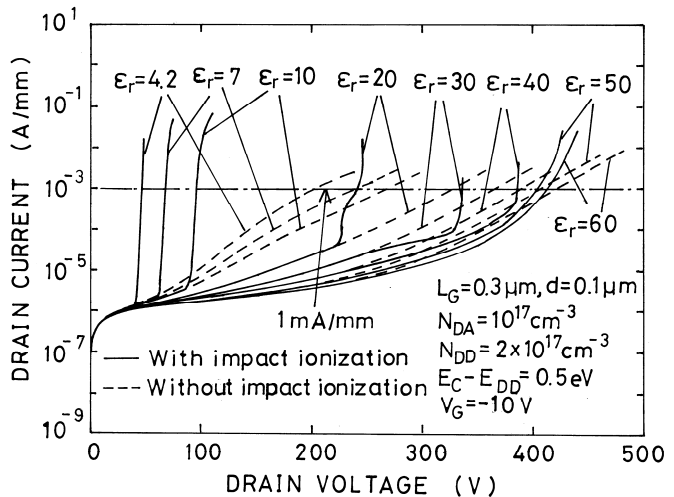


Figure 4: Calculated  $I_D - V_D$  curves of AlGaIn/GaN HEMTs as a parameter of  $\epsilon_r$ .  $V_G = -10$  V.  $L_{GD} = 1.5$   $\mu\text{m}$  and  $d = 0.1$   $\mu\text{m}$ .

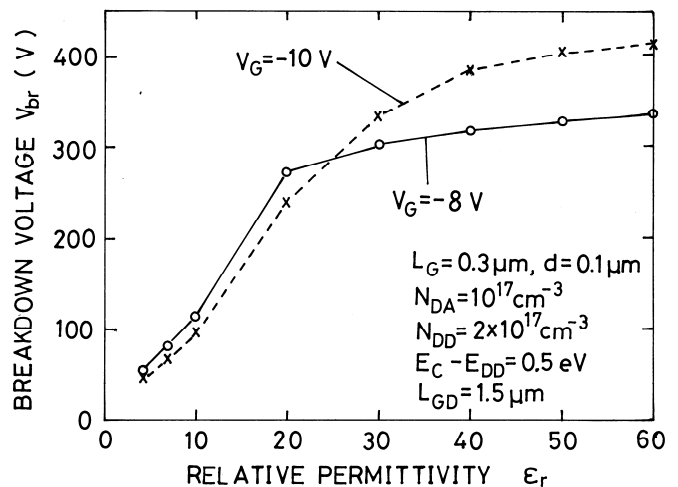


Figure 5: Calculated off-state breakdown voltage  $V_{br}$  versus  $\epsilon_r$  for different  $V_G$ .  $L_{GD} = 1.5$   $\mu\text{m}$  and  $d = 0.1$   $\mu\text{m}$ .

other hand, when  $\epsilon_r$  is high, the buffer leakage current reaches a critical value and determines the breakdown voltage before the impact ionization becomes a problem. And the breakdown voltage becomes higher for higher  $\epsilon_r$ . It has also been shown that when the gate voltage becomes more negative, the breakdown voltage in the high  $\epsilon_r$  region increases because the buffer leakage current becomes smaller.

#### REFERENCES

- [1] U. K. Mishra, L. Shen, T. E. Kazior, and Y.-F. Wu, "GaN-based RF power devices and amplifiers", Proc. IEEE, vol.96, pp.287-305, 2008.

- [2] N. Ikeda, Y. Niiyama, H. Kambayashi, Y. Sato, T. Nomura, S. Kato, and S. Yoshida, "GaN power transistors on Si substrates for switching applications", Proc. IEEE, vol.98, pp.1151-1161, 2010.
- [3] Y. Ando, Y. Okamoto, H. Miyamoto, T. Nakayama, T. Inoue, and M. Kuzuhara, "10-W/mm AlGaIn/GaN HFET with a field modulating plate," IEEE Electron Device Lett., vol. 24, pp. 289–291, 2003.
- [4] Y.-F. Wu, A. Saxler, M. Moore, R. P. Smith, S. Sheppard, P. M. Chavarkar, T. Wisleder, U. K. Mishra, and P. Parikh, "30-W/mm GaN HEMTs by field plate optimization", IEEE Electron Device Lett., vol.25, pp.117-119, 2004.
- [5] Y. Hao, L. Yang, X. Ma, J. Ma, M. Cao, C. Pan, C. Wang, and I. Zhang, "High-performance microwave gate-recessed AlGaIn/AlN/GaN MOS-HEMT with 73% power-added efficiency", IEEE Electron Device Lett., vol.32, pp.626-628, 2011.
- [6] A. Brannick, N. A. Zakhleniuk, B. K. Ridley, J. R. Shealy, W. J. Schaff, and L. F. Eastman, "Influence of field plate on the transient operation of the AlGaIn/GaN HEMT", IEEE Electron Device Lett., vol.30, pp.436-438, 2009.
- [7] K. Horio, A. Nakajima, and K. Itagaki, "Analysis of field-plate effects on buffer-related lag phenomena and current collapse in GaN MESFETs and AlGaIn/GaN HEMTs", Semicond. Sci. Technol., vol.24, pp.085022-1–085022-7, 2009.
- [8] S. Karmalkar and U. K. Mishra, "Enhancement of breakdown voltage in AlGaIn/GaN high electron mobility transistors using a field plate", IEEE Trans. Electron Devices, vol.48, pp.1515-1521, 2001.
- [9] E. Bahat-Treidel, O. Hilt, F. Brunner, V. Sidorov, J. Würfl, and G. Tränkle, "AlGaIn/GaN/AlGaIn DH-HEMTs breakdown voltage enhancement using multiple gating field plates (MGFPs)", IEEE Trans. Electron Devices, vol.57, pp.1208-1216, 2010.
- [10] H. Onodera and K. Horio, "Analysis of buffer-impurity and field-plate effects on breakdown characteristics in small sized AlGaIn/GaN high electron mobility transistors", Semicond. Sci. Technol., vol.27, pp.085016-1–085016-6, 2012.
- [11] H. Hanawa and K. Horio, "Increase in breakdown voltage of AlGaIn/GaN HEMTs with a high- $k$  dielectric layer", Phys. Status Solidi A, vol.211, pp.784-787, 2014.
- [12] H. Hanawa, H. Onodera, A. Nakajima, and K. Horio, "Numerical analysis of breakdown voltage enhancement in AlGaIn/GaN HEMTs with a high- $k$  passivation layer", IEEE Trans. Electron Devices, vol.61, pp.769-775, 2014.
- [13] Q. Luo and Q. Yu, "Electric field modulation by introducing a  $HK$  dielectric film of tens of nanometers in AlGaIn/GaN HEMT", Nanosci. Nanotechnol. Lett., vol.4, pp.936-939, 2012.
- [14] C. Liu, E. F. Chor, and L. S. Tan, "Enhanced device performance of AlGaIn/GaN HEMTs using HfO<sub>2</sub> high- $k$  dielectric for surface passivation and gate oxide", Semicond. Sci. Technol., vol.22, pp.522-527, 2007.
- [15] S. Yang, S. Huang, H. Chen, C. Zhou, Q. Zhou, M. Schnee, Q. Zhao, J. Schubert, and K. J. Chen, "AlGaIn/GaN MISHEMTs with high- $k$  LaLuO<sub>3</sub> gate dielectric", IEEE Electron Device Lett., vol.33, pp.979-981, 2012.
- [16] K. Horio, K. Yonemoto, H. Takayanagi, and H. Nakano, "Physics-based simulation of buffer-trapping effects on slow current transients and current collapse in GaN field effect transistors", J. Appl. Phys., vol.98, pp.124502-1–124502-7, 2005.
- [17] K. Horio and A. Nakajima, "Physical mechanism of buffer-related current transients and current slump in AlGaIn/GaN high electron mobility transistors", Jpn. J. Appl. Phys., vol.47, pp.3428-3433, 2008.
- [18] K. Horio, H. Onodera, and A. Nakajima, "Analysis of backside-electrode and gate-field-plate effects on buffer-related current collapse in AlGaIn/GaN high electron mobility transistors", J. Appl. Phys., vol.109, pp.114508-1–114508-7, 2011.
- [19] M. J. Uren, K. J. Nash, R. S. Balmer, T. Martin, E. Morvan, N. Caillas, S. L. Delage, D. Ducatteau, B. Grimbert, and J. C. De Jaeger, "Punch-through in short-channel AlGaIn/GaN HFETs", IEEE Trans. Electron Devices, vol.53, pp.395-398, 2006.
- [20] K. Horio and K. Satoh, "Two-dimensional analysis of substrate-related kink phenomena in GaAs MESFET's", IEEE Trans. Electron Devices, vol.41, pp.2256-2261, 1994.
- [21] Y. Mitani, D. Kasai and K. Horio, "Analysis of surface-state and impact-ionization effects on breakdown characteristics and gate-lag phenomena in narrowly-recessed-gate GaAs FETs", IEEE Trans. Electron Devices, vol.50, pp.285-291, 2003.
- [22] Y. Kazami, D. Kasai and K. Horio, "Numerical analysis of slow current transients and power compression in GaAs FETs", IEEE Trans. Electron Devices, vol.51, pp.1760-1764, 2004.
- [23] C. Bulutay, "Electron initiated impact ionization in AlGaIn alloys", Semicond. Sci. Technol., vol.17, pp.59-62, 2002.
- [24] K. Horio, H. Yanai and T. Ikoma, "Numerical simulation of GaAs MESFET's on the semi-insulating substrate compensated by deep traps", IEEE Trans. Electron Devices, vol.35, pp.1778-1785, 1988.
- [25] K. Horio, K. Asada and H. Yanai, "Two-dimensional simulation of GaAs MESFETs with deep acceptors in the semi-insulating substrate", Solid-State Electron., vol.34, pp.335-343, 1991.